INTERNATIONAL JOURNAL FOR NUMERICAL METHODS IN FLUIDS, VOL. 7, 215–231 (1987)

FINITE ELEMENT ANALYSIS OF FLOW IN A GAS-FILLED ROTATING ANNULUS*

M. H. BERGER

The Oak Ridge National Laboratory, POB X, Bldg X1000, MS332, Oak Ridge, Tennessee 37831-6332, U.S.A.

SUMMARY

Linearized multidimensional flow in a gas centrifuge can be described away from the ends by Onsager's pancake equation. However a rotating annulus results in a slightly different set of boundary conditions from the usual symmetry at the axis of rotation. The problem on an annulus becomes ill-posed and requires some special attention. Herein we treat axially linear inner and outer rotor temperature distributions and velocity slip. An existence condition for a class of non-trivial, one-dimensional solutions is given. New exact solutions in the infinite bowl approximation have been derived containing terms that are important at finite gap width and non-vanishing velocity slip. The usual one-dimensional, axially symmetric solution is obtained as a limit. Our previously reported finite element algorithm has been extended to treat this new class of problems. Effects of gap width, temperature and slip conditions are illustrated. Lastly, we report on the compressible, finite length, circular Couette flow for the first time.

KEY WORDS Finite Element Method Rotating Fluid Mechanics Slip Flow

INTRODUCTION

We are interested in computing the steady, internal flow in a rotating annulus containing a gas, say uranium-hexafluoride (UF_6). See Figure 1 for a conceptual sketch.

Incompressible flow between two infinity long rotating cylinders is a classical fluid mechanics problem which leads to a simple exact solution of the Navier–Stokes equations.[1] Concentric cylinders have been used in the study of fluid stability theories for incompressible, circular Couette flows as well. Taylor vortices or roll cells are produced in the incompressible regime under unstable conditions.[1,2] This has been the subject of numerous recent theoretical and experimental efforts.[3–5] Also, the problem of atmospheric stability is related to the thermal convection in a rotating annulus.[2]

Unstable modes can occur when the inner surface rotates faster than the outer surface or a thermal inversion exists. Under some conditions of gap width, Reynolds number, etc. a compressible fluid may also exhibit Taylor vortices. Neither theoretical, numerical nor experimental studies of the compressible Taylor problem have been reported. Furthermore, transition and ultimately turbulent flow might occur which would be devastating for isotope separation.

In a recent numerical examination of viscous, incompressible rotating flows using the finite element method, Reference 6 reported a velocity vector plot for the circulation due to a stable

* Based on work performed at Oak Ridge Gaseous Diffusion Plant, operated by Martin Marietta Energy Systems, Inc, for the U.S. Department of Energy under U.S. Government contract DE-AC05-840R21400.

0271–2091/87/030215–17$08.50

Received 29 January 1986
Revised 16 July 1986

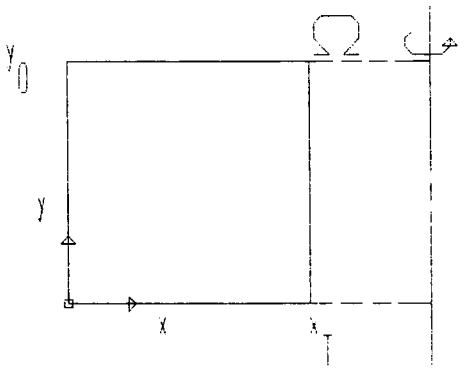

Figure 1. Rotating gas filled annulus

differential rotation (i.e. stationary inner rotor). Several more recent numerical and experimental works have been reported for concentric cylinders and concentric spheres.[7,8] At the start of our work (Circa 1982), to the best of our knowledge the class of problems associated with the internal fluid dynamics of a rotating annulus containing a compressible, viscous, heat conducting fluid had not been analysed in detail. Our model is subject to the limitations of linearized, steady-state fluid mechanics as governed by Onsager's pancake equation[9] for the vertical boundary layer and the Carrier–Maslen end conditions[10] for the horizontal boundary layers. The Galerkin finite element method is used to simultaneously solve our sixth order partial differential equation and boundary conditions. We derive some new, exact, uniformly valid analytical solutions for simple axially linear inner and outer rotor temperature distributions. Also, we report results for finite length, compressible circular Couette flow after establishing the validity of the pancake equation for these new applications.

Since 1982, Conlisk and coworkers published several papers along similar lines. First they considered the effect of a mass source/sink on a Boussinesq-type fluid in a rotating annulus.[11] Then they extended this to a model annular gas centrifuge with differentially rotating end-caps, different uniform rotor temperatures, with feed and withdrawal taken at three corners of the machine.[12] More recently, they made claims that theirs is the first self-consistent theory of flow and mass transfer in a gas centrifuge.[13] Feed through axisymmetric ports in the rotor walls was included and a special point was made of the specified boundary condition for the isotope separation theory. The separation process was quantified by a scaled end-to-end separation factor. We simply note that for pure thermal drive in the long bowl limit for no slip at x_T (see 'Exact solution' section), it can be shown that

$$E \sim \frac{108(x_T - 4)^2}{A^2(15x_T^2 - 112x_T + 212)}, \tag{1}$$

where E is Cohen's E based on the maximum theoretical separative work of the outer rotor.[14] Of course, this reduces to the usual $7{\cdot}2/A^2$ for $x_T \to \infty$.[15]

PERTURBATION THEORY

The derivation of Onsager's equation from the linearized Navier–Stokes equations using order-of-magnitude considerations[16] or more formal asymptotic expansions[17] involves the boundary layer co-ordinate x. This is so-called scale heights variable, which we define as $x \sim 2A^2(1-\eta)$, where η is the normalized radial co-ordinate, $0 \leqslant \eta \leqslant 1$. In the usual asymptotic theory, $A \to \infty$ so that

$0 \leqslant x \leqslant \infty$. But to reduce the computational domain we substitute $0 \leqslant x \leqslant x_T$, for arbitrarily large x_T. However, for an annulus, $0 \leqslant \eta_i \leqslant \eta \leqslant 1$, but $A \to \infty$ so that apparently $0 \leqslant x \leqslant \infty$ is again obtained and x fails to sense η_i. Suppose[18] $x_T = 2A^2(1-\eta_i)$. This can be formally justified via perturbation theory by defining the gap width δ, $\delta = 1-\eta_i$, such that, $2A^2\delta = O(x_T)$.

Now when limits are taken in which the stratification parameter, A, goes to infinity, the gap width goes as its inverse. This introduces the further limitation of a 'small' gap, $\delta \ll 1$, or, $\eta_i \simeq 1$. Thus, by construction,

$$\lim_{\eta \to \eta_i, A^2 \to \infty; \text{ with } 2A^2\delta = O(x_T)} x = x_T. \tag{2}$$

Therefore the previous asymptotic derivations of the inner–outer expansion and inner–inner expansion[17] carry over with the additional similarity rule. It is these equations which lead to Onsager's equation and the Carrier–Maslen end conditions for a rotating annulus. The appropriate boundary conditions take some further consideration.

GOVERNING EQUATION AND BOUNDARY CONDITIONS

Linearized flow in a gas-filled rotating *annulus* may be described away from the ends by Onsager's so-called 'Pancake' equation, written in operator form as

$$L\chi = L_6\chi + B^2\chi_{yy} = F^*(x, y), \tag{3}$$

where χ is the master potential with $0 \leqslant x \leqslant x_T$ and

$$L_6\chi = [e^x(e^x\chi_{xx})_{xx}]_{xx} \tag{4}$$

subject to eight boundary conditions:

$$\chi_x(0, y) = \chi_{xx}(0, y) = 0, \quad L_5\chi(0, y) = \frac{Re}{32A^{10}}\bar{\theta}_y(0, y),$$

$$\chi_x(x_T, y) = \beta e^{x_T}\chi_{xx}(x_T, y) + L_3\chi(\infty, y) = 0,$$

$$L_5\chi(x_T, y) = \frac{Re}{32A^{10}}\bar{\theta}_y(x_T, y),$$

$$\chi_y(x, 0) = -4S^{-1/4}Re^{-1/2}A^4[e^{x/2}\chi_x(x, 0)]_x,$$

$$\chi_y(x, y_0) = 4S^{-1/4}Re^{-1/2}A^4[e^{x/2}\chi_x(x, y_0)]_x. \tag{5}$$

Note that the source/sink term $F^*(x, y)$ may be different from $F(x, y)$ in a simple rotating cylinder.[16] Following a physical or heuristic approach one might simply invoke the same specifications at $x = x_T$ as at $x = 0$. That is

$$\chi_x(x_T, y) = \chi_{xx}(x_T, y) = 0. \tag{6}$$

However, we take a formalistic approach and derive the conditions written earlier (equation (5)) from the weak formulation.

WEAK FORMULATION

One of the so-called 'virtues' of the finite element method is the case of changing boundary conditions.[19] The new boundary conditions (equations (5) or (6)) and boundaries analysed here require the computation of the three eigenfunctions discarded by Onsager and followers.[16] Also

the eigenvalues have to be recomputed. Perhaps some crude measurement of this effort can be taken from the one-dimensional example in the next section, 'Exact Solution'.

In the finite element method we simply retain some additional boundary contributions (natural boundary conditions and load vectors) at x_T that were previously discarded and modify a few essential boundary conditions. Such changes amount to a relatively modest chore.

General derivation

The method of weighted residuals requires satisfaction of the vanishing of the weighted residual. In other words

$$-(\omega, L\chi - F) = 0 \tag{7}$$

over the x, y domain Γ with boundary $\partial\Gamma$. Formally integrating by parts thrice on x and once on y produces

$$\iint_{\Gamma} [L_3\omega L_3\chi + B^2\omega_y\chi_y + F\omega]\mathrm{d}x\mathrm{d}y$$
$$+ \int_{\partial\Gamma} [\mathrm{e}^x\omega_x L_4\chi - \mathrm{e}^x\omega_{xx}L_3\chi - \omega L_5\chi]|_{x=0}^{x_T}\mathrm{d}y - B^2\int_{\partial\Gamma}\omega\chi_y|_{y=0}^{y_0}\mathrm{d}x = 0. \tag{8}$$

Upper atmosphere natural boundary conditions at x_T obviously involve $L_5\chi, \omega_{xx}, L_3\chi, L_4\chi, \omega_x$. We treat only the first three boundary conditions. The fourth condition involves a high-order derivative which has no immediate physical importance and the last term relates to non-zero throughput. The most interesting non-homogeneous boundary conditions at x_T are $L_5\chi$ and $L_3\chi$.

Generalized slip

For a sufficiently large gap, say $x_T = 15$, and stratification, A, the local wheel flow may indicate rarefied flow near x_T such that the local Knudsen number is approximately 1. It is well known that under rarefied conditions gas behaviour changes and slip occurs.[20] That is, fluid can no longer adhere to a solid surface but has some finite, non-zero slip velocity. Likewise a temperature slip, jump or discontinuity may occur. For simplicity, we assume axial slip in the absence of any azimuthal velocity slip or temperature jump.

Rigorous determination of the slip flow is quite difficult and involves the solution of Boltzmann's equation for the molecule distribution function. An alternative formulation for the molecular flow gives a model Kramer's problem involving an integral equation modified to account for exponential stratification.[21] Although this is an equally interesting problem area, we shall not delve further into the thin air of rarefied gas dynamics. Instead we constrain ourselves to a macroscopic parametrization of slip.

The chosen class of problems is defined by boundary conditions in some arbitrary specified axial rotor temperature distribution (or temperature gradient) and axial slip parameter. We will not address internal sources and sinks either. Discretizing χ, considering a vector of local weight functions $\mathbf{w}^e$, and choosing $\mathbf{w}^e$ to be the same as $\mathbf{N}^e$ yields the Galerkin method. Bold characters designate column vectors and bold characters in square brackets denote matrices. Introducing the Ekman boundary layer suction conditions into the boundary integrals over the horizontal rotating surfaces and appropriately integrating by parts, using the boundary conditions

$$\chi_x(0, y) = \chi_x(x_T, y) = 0 \tag{9}$$

equation (8) becomes

$$\sum_e \int\int_{\Gamma^e} [(L_3\mathbf{N}^e L_3\mathbf{N}^{eT} + B^2\mathbf{N}_y^e\mathbf{N}_y^{eT})\mathbf{u}^e + F^e\mathbf{N}^e]\,dx\,dy$$
$$+ \sum_e \frac{Re}{32A^{10}} \int_{\partial\Gamma^e} [\bar{\theta}_y(0,y)\mathbf{N}^e(0,y) - \bar{\theta}_y(x_T,y)\mathbf{N}^e(x_T,y)]dy$$
$$+ \sum_e [4B^2S^{-1/4}Re^{-1/2}A^4 \int_{\partial\Gamma^e} [e^{x/2}\mathbf{N}_x^e(x,y_0)\mathbf{N}_x^{eT}(x,y_0)$$
$$+ e^{x/2}\mathbf{N}_x^e(x,0)\mathbf{N}_x^{eT}(x,0)]\,dx - e^{x_T}\int_{\partial\Gamma^e} \mathbf{N}_{xx}^e(x_T,y)L_3\mathbf{N}^e(x_T,y)^T\,dy]\mathbf{u}^e = \mathbf{0}. \tag{10}$$

$\mathbf{N}^e$ is the local basis and $\mathbf{u}^e$ is the discretization of χ over an elementary subdomain involving nodal values and derivatives of χ. This is just the usual numerical linear algebra problem

$$\sum_e ([\mathbf{K}^e]\mathbf{u}^e - \mathbf{f}^e) = \mathbf{0}. \tag{11}$$

The two matrices evaluated at x_T are new. The system equations are subject to the essential boundary conditions,

$$\chi_x(0,y) = \chi_{xx}(0,y) = \chi_x(x_T,y) = 0. \tag{12}$$

Classical continuum mechanics treats fluid flow with slip, whether it is at an interface of two fluids[22,23] or a rarefied gas,[24] by assuming that the slip velocity is simply proportional to the transverse shear:

$$\beta'' w + \mu\frac{\partial w}{\partial n} = 0, \tag{13}$$

where μ is the absolute viscosity, β'' is the dimensional slip coefficient, w is the dimensional velocity (used elsewhere it is the usual perturbation velocity) and n is measured normal to the boundary. In the terminology of partial differential equation theory, this is just a boundary condition of the third kind or Robin's type. Here β'' plays a role similar to the film coefficient in Newton's cooling law, from the theory of heat conduction, and β''/μ parametrizes slip. The appropriate non-dimensional form of equation (13) for this application is

$$\beta e^{x_T}\chi_{xx}(x_T,y) + L_3\chi(x_T,y) = 0, \tag{14}$$

where β is the dimensionless slip coefficient, defined as

$$\beta = \frac{\beta' Re}{2A^2}, \tag{15}$$

and β' is the simple dimensionless slip coefficient associated with β''. Equation (14) degenerates to no slip for $\beta \to \infty$ and gives free slip in the limit $\beta \to 0$. Intermediate positive values of β correspond to finite slippage. Thus

$$[\mathbf{K}_b^e(x_T)] = \beta e^{2x_T}\int \mathbf{N}_{xx}^e(x_T,y)\mathbf{N}_{xx}^e(x_T,y)^T dy, \tag{16}$$

where the natural boundary condition at x_T has already been included. For regular, right circular cylindrical domains one can use outer product basis functions defined on rectangles, such as $\mathbf{H}_3^e(\eta)$ and $\mathbf{H}_5^e(\xi)$ where[17]

$$\mathbf{H}_3^e(\eta) = \begin{Bmatrix} (2-3\eta+\eta^3)/4 \\ (1-\eta-\eta^2+\eta^3)l_y^e/8 \\ (2+3\eta-\eta^3)/4 \\ (1-\eta+\eta^2+\eta^3)l_y^e/8 \end{Bmatrix},$$

$$\mathbf{H}_5^e(\xi) = \begin{Bmatrix} (1-\xi)^3(3\xi^3+9\xi+8)/16 \\ (1+\xi)(1-\xi)^3(3\xi+5)l_x^e/32 \\ (1+\xi)^2(1-\xi)^3 l_x^{e2}/64 \\ (1+\xi)^3(3\xi^3-9\xi+8)/16 \\ (1+\xi)^3(1-\xi)(3\xi-5)l_x^e/32 \\ (1+\xi)^3(1-\xi)^2 l_x^{e2}/64 \end{Bmatrix}. \tag{17}$$

with the chosen tensor product basis, $\mathbf{N}^e(\xi,\eta) = \mathbf{H}_5^e(\xi) \otimes \mathbf{H}_3^e(\eta)$, it is necessary to impose additional constraints on the mixed derivatives at the side walls, say

$$\chi_{xy}(0,y) = \chi_{xxy}(0,y) = \chi_{xy}(x_T,y) = 0. \tag{18}$$

Still the problem is indeterminate, or determind to within an arbitrary additive constant, because we have lost the usual Dirichlet condition, $\chi(\infty,y) = 0$. Notice that antisymmetrical flow problems must exhibit $\chi(x, y_0/2) = 0$. In general, to pin down the potential and make the problem well-posed, suppose $\chi(x_T, y_0/2) = 0$.

EXACT SOLUTION

In the limit $y \to \infty$ such that $\partial/\partial y(\ ) = 0$ we obtain the so-called long bowl model equation which can be solved exactly. Thus

$$L_6\chi = 0 \tag{19}$$

for $F^*(x) = 0$, subject to the boundary conditions

$$\chi'(0) = \chi''(0) = 0, L_5\chi(0) = c_1, \text{ constant}$$
$$\chi(x_T) = \chi'(x_T) = \beta e^{x_T}\chi''(x_T) + L_3\chi(x_T) = 0, L_5\chi(x_T) = c_2, \text{ constant} \tag{20}$$

We can use superpositioning of the separate temperature inhomogeneities since the equation system is linear. Equation (19) can be integrated straightforwardly six times to yield the general solution

$$\chi(x) = -a_1[\tfrac{1}{4}(x+3)e^{-2x}] + \frac{a_2}{4}e^{-2x} + a_3(x+2)e^{-x} + a_4e^{-x} + a_5x + a_6. \tag{21}$$

However, existence of one-dimensional, axially invariant flow requires that $c_1 = c_2$, say a_1. Application of these boundary conditions gives

$$\chi''(0) = 2a_1 + a_2 + a_4 = 0,$$

$$\chi'(0) = -\frac{5a_1}{4} - \frac{a_2}{2} - a_3 - a_4 + a_5 = 0,$$

$$\beta e^{x_T}\chi''(x_T) + L_3\chi(x_T) = \beta\{[a_1(x_T+2)+a_2]e^{-x_T} + a_3x_T + a_4\}$$
$$+ [-a_1(x_T+1)e^{-x_T} - a_2e^{-x_T} + a_3] = 0,$$

$$\chi'(x_T) = -\tfrac{1}{2}[a_1(x_T+\tfrac{5}{2})+a_2]e^{-2x_T} - a_3(x_T+1)e^{-x_T} - a_4 e^{-x_T} + a_5 = 0, \tag{22}$$

$$\chi(x_T) = a_1[\tfrac{1}{4}(x_T+3)e^{-2x_T}] + \frac{a_2}{4}e^{-2x_T} + a_3(x_T+2)e^{-x_T} + a_4 e^{-x_T} + a_5 x_T + a_6 = 0.$$

This 4×4 matrix problem gives, after much algebra,

$$a_2 = \frac{a_1}{\mathrm{DET}}\{2\beta - \tfrac{3}{4}(\beta x_T+1) + [(1-2\beta)(x_T+1) + (2\beta x_T+1) - \beta(x_T+2)]e^{-x_T} - [\tfrac{1}{2}(\beta x_T+1)(x_T+\tfrac{5}{2}) + (x_T+1)[(x_T+1) - \beta(x_T+2)]]e^{-2x_T}\},$$

$$a_3 = \frac{a_1}{\mathrm{DET}}\left\{\frac{\beta}{4} + [\tfrac{3}{4}(\beta-1) + \frac{(x_T+1)}{2} - \frac{\beta}{2}(x_T+2)]e^{-x_T} + [2 - \frac{\beta}{2}(x_T+\tfrac{9}{2}) - (x_T+1) + \beta(x_T+2)]e^{-2x_T} + \tfrac{1}{2}[(\beta-1)(x_T+\tfrac{5}{2}) + (x_T+1) - \beta(x_T+2)]e^{-3x_T}\right\},$$

$$a_4 = \frac{a_1}{\mathrm{DET}}\{-\tfrac{1}{4}(\beta x_T+1) - [2(\beta-1) + (x_T+1) - \beta(x_T+2)]e^{-x_T} + [-(\beta x_T+1) + 2(x_T+1)(\beta-1) + \tfrac{1}{2}(\beta x_T+1)(x_T+\tfrac{5}{2}) + (x_T+1)[(x_T+1) - \beta(x_T+2)]]e^{-2x_T}\},$$

where the determinant, DET, is

$$\mathrm{DET} = \beta[(x_T+1)e^{-x_T} - 1] - \tfrac{1}{2}(1-e^{-2x_T})(\beta x_T+1) - (e^{-x_T}-1)(\beta x_T+1) - (\beta-1)e^{-x_T}[(x_T+1)e^{-x_T} - 1]. \tag{23}$$

Use of an algebraic manipulation code to invert the coefficient matrix is preferable to longhand. Let $x_T > 1$, so that $e^{-2x_T} \ll 1$, then

$$\mathrm{DET} \sim \beta[(x_T+1)e^{-x_T} - 1] + (\tfrac{1}{2} - e^{-x_T})(\beta x_T+1) + (\beta-1)e^{-x_T}.$$

$$a_2 \sim \frac{a_1}{\mathrm{DET}}\{2\beta - \tfrac{3}{4}(\beta x_T+1) + [(1-2\beta)(x_T+1) + (2\beta x_T+1) - \beta(x_T+2)]e^{-x_T}\},$$

$$a_3 \sim \frac{a_1}{\mathrm{DET}}\left\{\frac{\beta}{4} + [\tfrac{3}{4}(\beta-1) + \frac{(x_T+1)}{2} - \frac{\beta}{2}(x_T+2)]e^{-x_T}\right\},$$

$$a_4 \sim \frac{a_1}{\mathrm{DET}}\{-\tfrac{1}{4}(\beta x_T+1) - ([2(\beta-1) + (x_T+1) - \beta(x_T+2)]e^{-x_T}\}. \tag{24}$$

Further simplification with $x_T \gg 1$, so that $e^{-x_T} \ll 1$, yields

$$\mathrm{DET} \sim \tfrac{1}{2}\beta x_T, \quad a_2 \sim -\frac{3a_1}{2}, \quad a_3 \sim 0,$$
$$a_4 \sim -\frac{a_1}{2}, a_5 \sim 0, a_6 \sim 0. \tag{25}$$

EXACT CALCULATIONS

Here we present some graphs illustrating sensitivity to the gap width in the long bowl limit. Suppose

$$a_1 = L_5\chi(0) = -1. \tag{26}$$

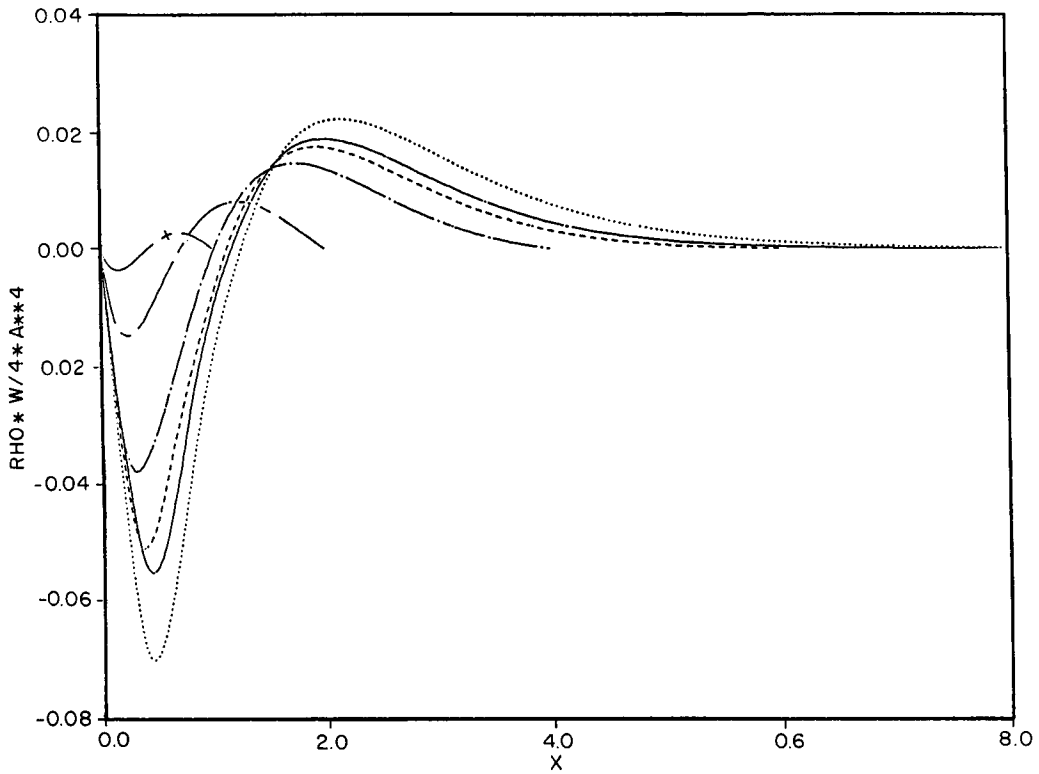

Figure 2. Effect of gap width on flow with no slip for $a_1 = -1$: ---- $x_T = \infty$; —— $x_T = 8$; ———— $x_T = 6$; —·—— $x_T = 4$; ———— $x_T = 2$; ——+—— $x_T = 1$

Physically, this corresponds to a unit strength, negative wall thermal gradient producing downflow at the outer rotor and upflow at the inner rotor. Figure 2 illustrates the effect of gap width on the flow with no slip for $1 \leqslant x_T \leqslant \infty$. The usual long bowl solution is recovered for $x_T \to \infty$, whereas significant differences exist for large, finite x_T, say 8 scale heights. Reduced rotor spacing obviously de-stratifies the gas and shifts the cross-over point, x_0, ever closer to the outer wall and concommitantly reduces the magnitude of the flow. For gaps of approximately 1 scale height, the countercurrent assumes a nearly antisymmetric appearance with $x_0 \simeq x_T/2$. Also, the flow no longer decays exponentially. Calculations for gap widths much less than 1/10 become quite difficult owing to the vanishing of the flow. Longer computer word lengths (e.g. quad precision) become necessary to compute the difference of almost equal terms.

Next, Figure 3 gives the flow for $x_T = \infty$, 10, 8, 6 and $a_1 = -1$ with free slip at the inner boundary. The only significant difference is for $x_T \leqslant 8$. Sensitivity to β is illustrated in Figure 4 for slip parameters covering three orders of magnitude including the intermediate range, with $x_T = 8$. Decreasing gap width tends to generally reduce the axial flow. As much as 20 per cent variation in the maximum velocity is evident. Clearly these solutions naturally lie between the limits of no slip and free slip and depend on only the slip parameter and not a detailed knowledge of the slip velocity.

FINITE ELEMENT NUMERICAL RESULTS

Consider the class of two-dimensional, pure boundary value problems for a finite length rotating

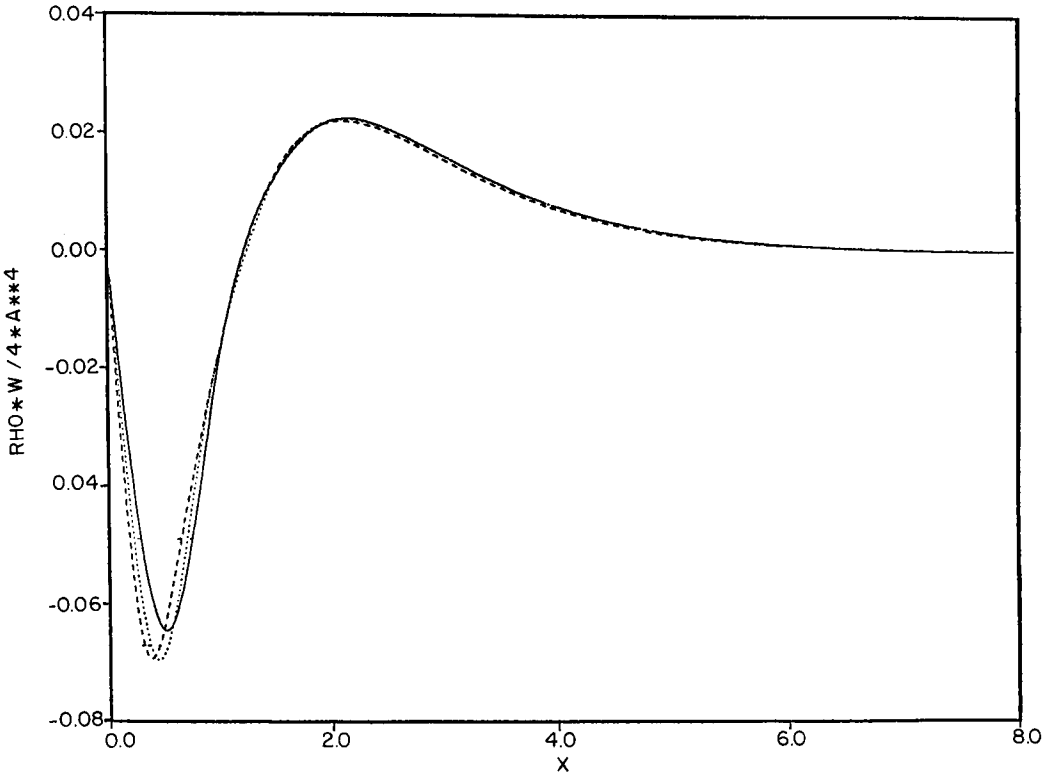

Figure 3. Effect of gap width on flow with free slip for $a_1 = -1$: —— $x_T = \infty$ and 10; - - - - $x_T = 8$; ———— $x_T = 6$

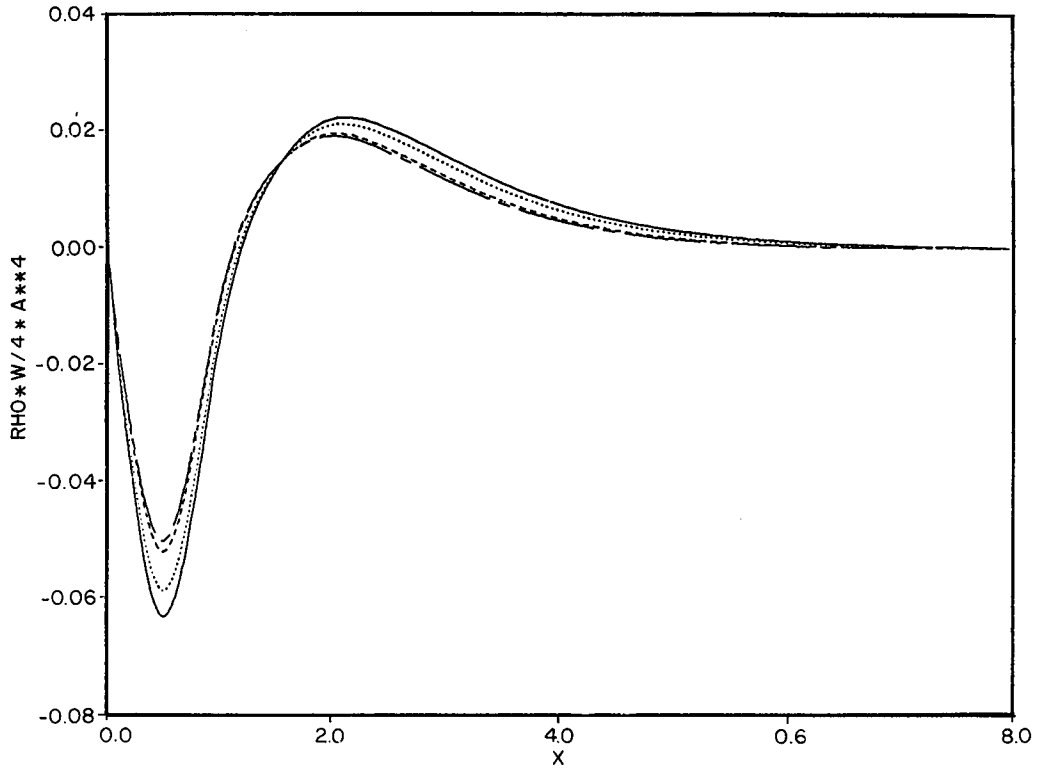

Figure 4. Effect of generalized slip parameter β on flow with $a_1 = -1$ and $x_T = 8$: ——— $\beta = 1/100$; - - - - $\beta = 1/10$; ———— $\beta = 1$; ———— $\beta = 10$

Table I. Gas centrifuge data[25]

a (radius)	0·09145 m	T_0 (temperature)	300 K
L (length)	3·353 m	V_w (rotor speed)	400, 500, 700 m/s

annulus such that $F^*(x, y) = 0$. These flows get their motivation from inhomogeneities on the vertical or horizontal surfaces. The special case of no slip at the inner rotor was computed using very large β (e.g. 10^{20}). For all the two-dimensional computations we specified a fixed, non-uniform computing grid with both axial and radial mesh refinements in the neighbourhood of the boundaries to resolve boundary layers. A uniform axial grid was used between the axially refined regions. Altogether, 168 elements involving 195 nodes (13 × 15) lead to 1170 simultaneous equations for the 24 degree of freedom element.

Thermal drive

Suppose that the thermal boundary conditions are identical along both inner and outer rotor walls. Let $\bar{\theta}_y$ be constant, so that the end-caps are in equilibrium with the local wall temperature. For calculational purposes consider the May machine[25] described by the data given in Table I. Say $p_w = 100$ torr (13330 N/m^2),[26] $V_w = 700$ m/s, $\Delta T = -1$K and $x_T = 8$.

Figure 5(a) gives the computed finite element approximation to the stream function on the half domain for no slip. The presence of the inner wall and new boundary conditions is most evident in the equipotential lines. Figure 5(b) gives the axial mass velocity distribution. Varying the slip parameter such that $\beta = 1$ (intermediate value), 0 (free slip) we obtain the streamlines shown in Figure 6(a) and (b). Clearly the circulation increases with increasing slip (decreasing β), by as much as 10 per cent, which agrees with our long bowl observations (Figure 2). As in all these calculations, the flow patterns resemble one another, but slip leads to streamline penetration higher into the atmosphere and the locus of cross-over points moves radially inward.

Compressible circular Couette flow

Incompressible flow between infinitely long concentric rotating cylinders has the well known laminar flow solution for the azimuthal velocity[1].

$$v(r) = \frac{1}{r_0^2 - r_i^2}\left[r(\Omega_0 r_0^2 - \Omega_i r_i^2) - \frac{r_i^2 r_0^2}{r}(\Omega_0 - \Omega_i)\right]. \tag{27}$$

The last term in the square bracket is due solely to the differential rotation. The above formula also holds for a compressible fluid. However that cannot be said for the finite length, compressible, heat conducting flow, which has non-zero values for all three velocity components. Incompressible, finite length circular Couette flow has been used to verify more general analyses[6] and may be quite different from its compressible variant. Differential rotation can have several forms; end-caps may rotate synchronously with either the inner or outer wall. Either way the flow is antisymmetric about the midplane. Assume that $\Omega_0 = \Omega + \Delta\Omega$ and $\Omega_i = \Omega$ (nearly-rigid-body rotation), and a differential rotation of 1 Hz.

$$\Delta\bar{\omega} = \frac{2\pi(1)}{\Omega} = \frac{2\pi a}{V_w} = 2\pi\frac{0{\cdot}09145}{700}. \tag{28}$$

The outer rotor has excess spin for stable flow

$$\Delta\bar{\phi}_0 = \Delta\bar{\phi}_{x_T} = -2\Delta\bar{\omega} = -1{\cdot}6417065 \times 10^{-3}. \tag{29}$$

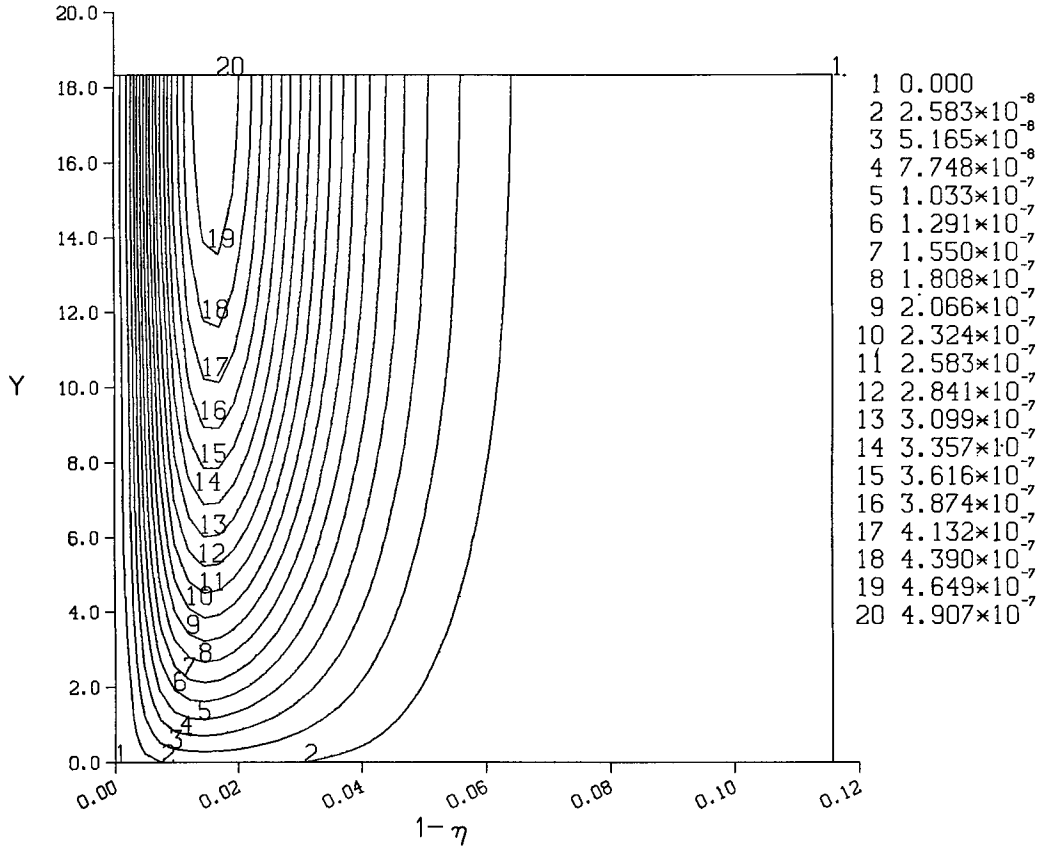

Figure 5(a). Thermal drive streamlines

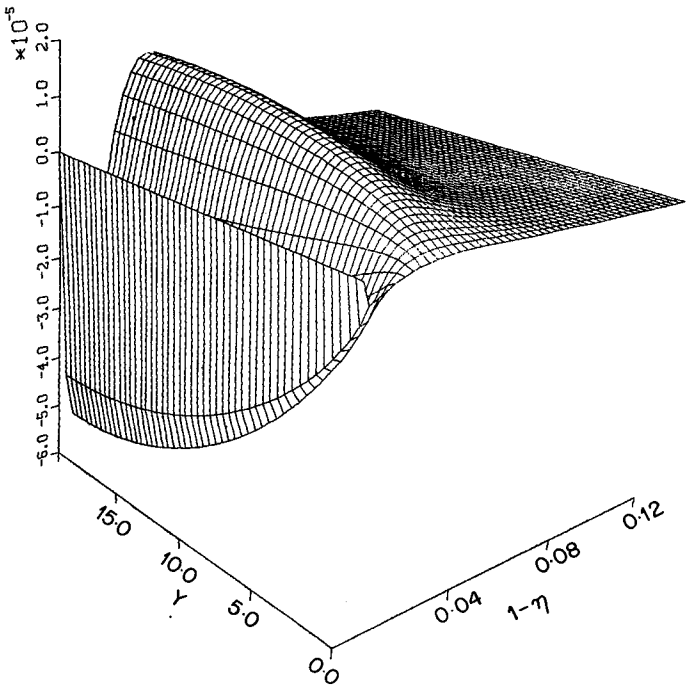

Figure 5(b). Three-dimensional plot of axial mass velocity for thermal drive

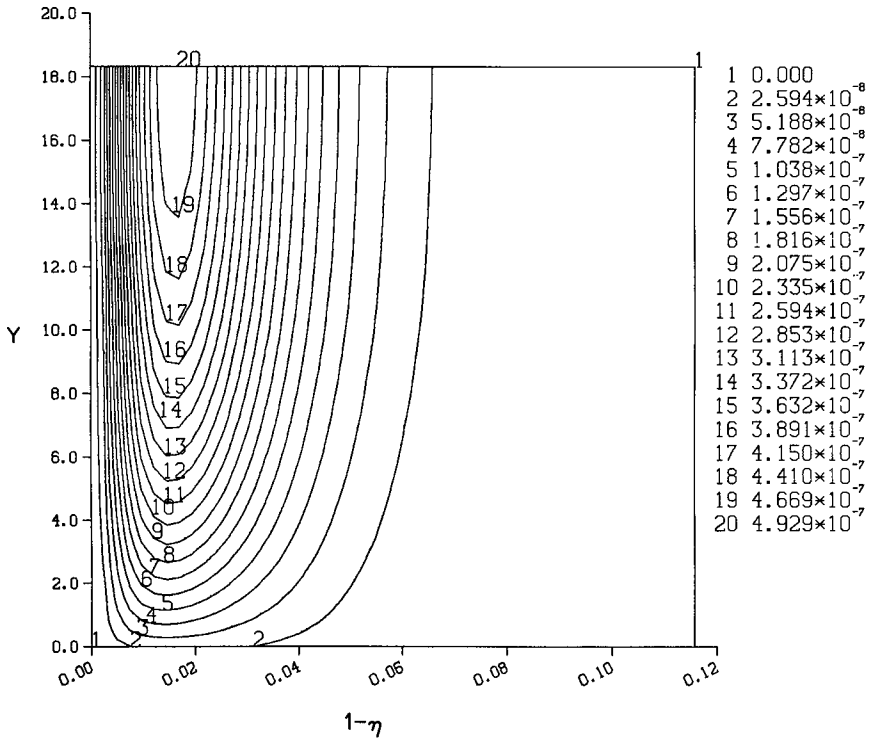

Figure 6(a). Thermal drive streamlines for intermediate slip

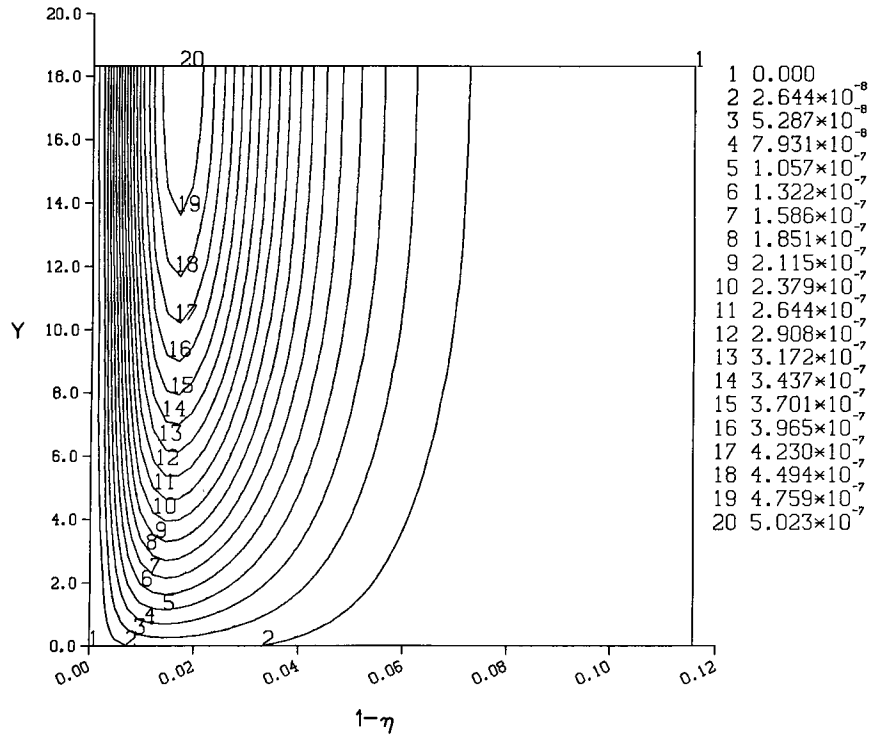

Figure 6(b). Thermal drive streamlines for free slip

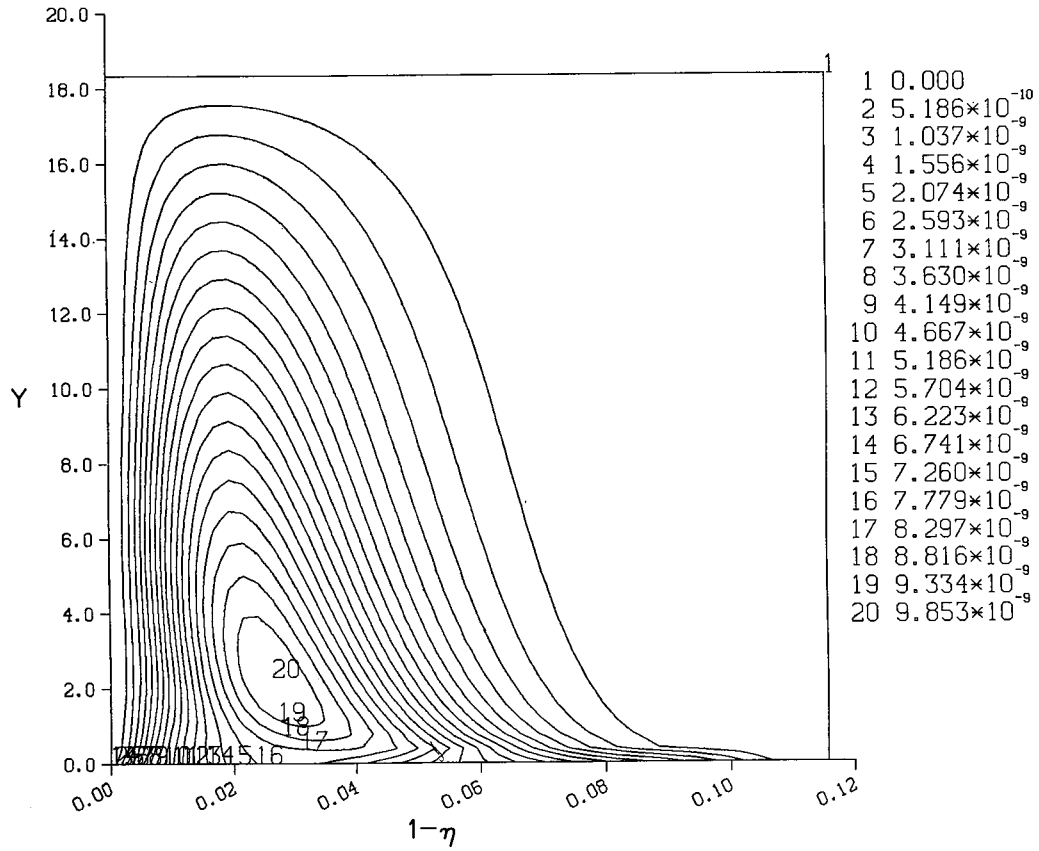

Figure 7(a). Circular Couette flow streamlines with discontinuity at x_T

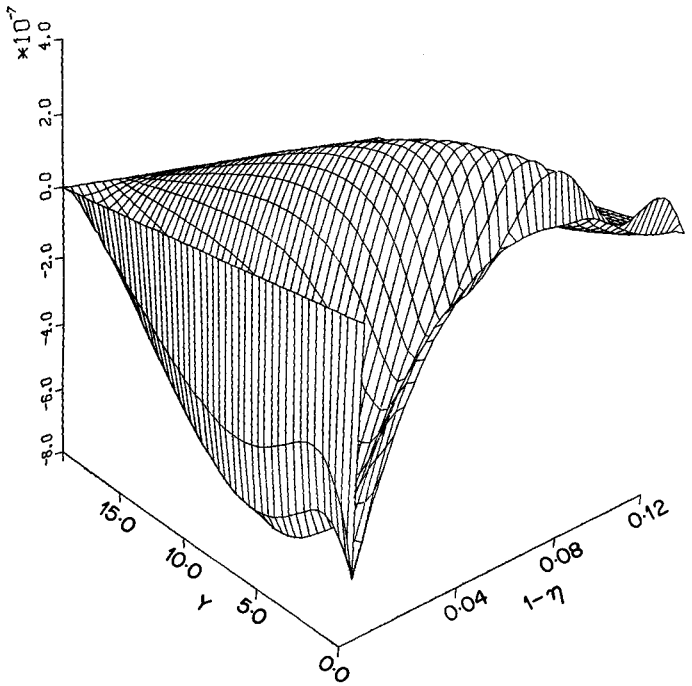

Figure 7(b). Three-dimensional plot of axial mass velocity for circular Couette flow with discontinuity at x_T

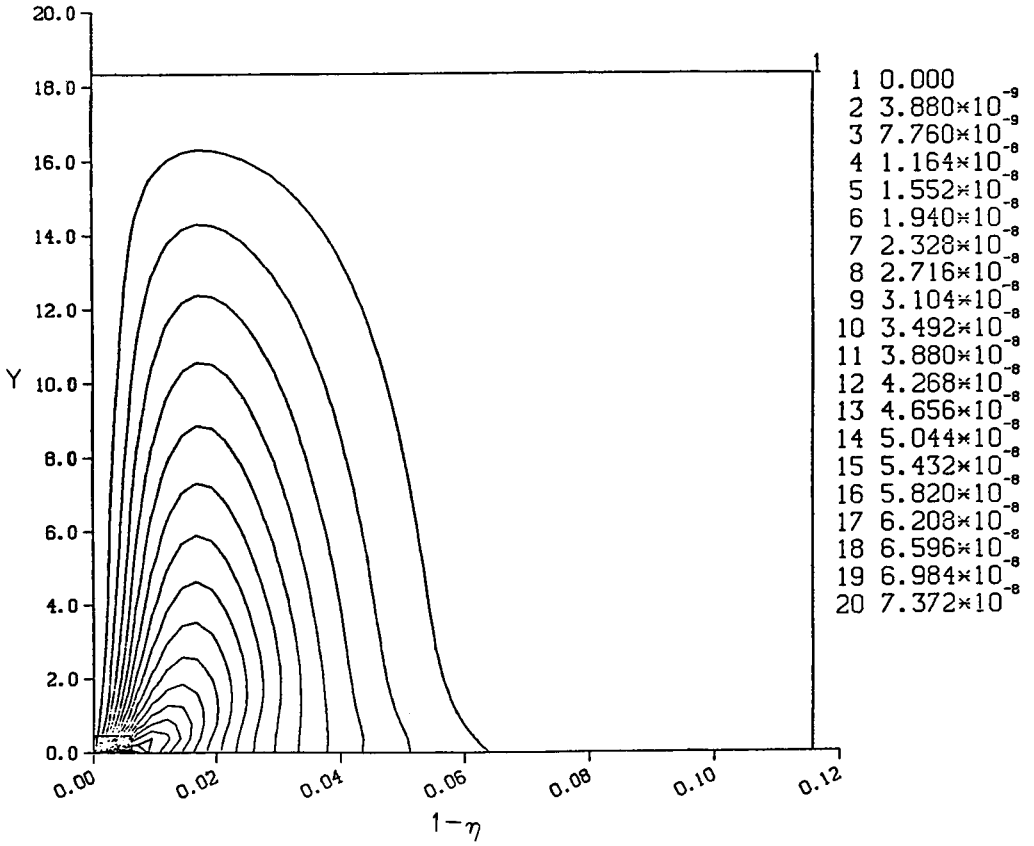

Figure 8(a). False Taylor flow streamlines with discontinuity at $x = 0$

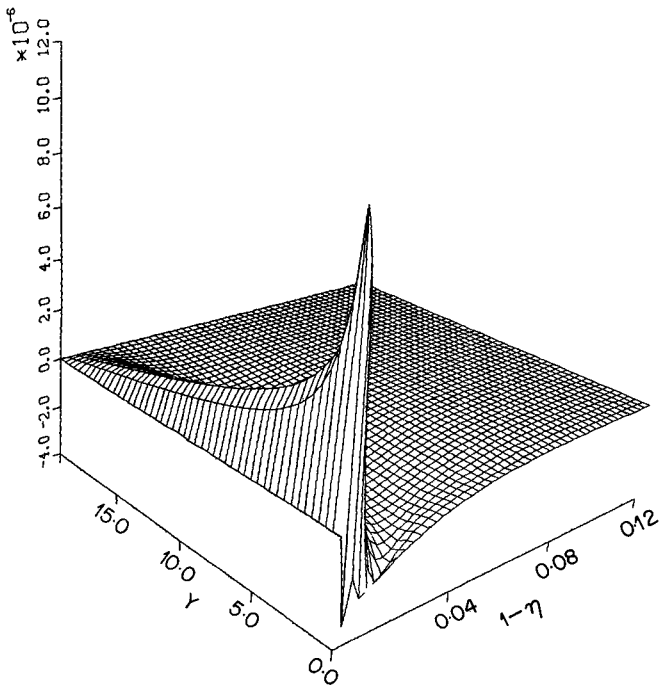

Figure 8(b). Three-dimensional plot of axial mass velocity for false Taylor flow with discontinuity at $x = 0$

A 1Hz differential spin is comparable to a 1K differential temperature. For $\Omega_{end} = \Omega_0$ the corner singularity is at x_T and the streamlines and axial flow are as given in Figures 7(a) and (b). Flow near the outer rotor is downward in the bottom of the machine. The discontinuity at $x = 0$ creates a much stronger counterclockwise circulation due to the exponential stratification. Strong Ekman pumping is exhibited with most of the flow going through the end Ekman boundary layers. Similar results hold for differential rotor temperatures. To our knowledge, this is the first solution to the compressible, finite length, pure circular Couette flow. Figure 7(a) resembles the two-cell meridional velocity field of the incompressible analogue[6]. In closing we observe that, instead of the Taylor instability, pancake theory predicts the reverse stable secondary flow if the sign of $\Delta\Omega$ is reversed, that is, a false Taylor flow (Figures 8(a) and (b)).

ACKNOWLEDGEMENT

The author sincerely thanks Dr. W. K. Sartory, The Oak Ridge National Laboratory, for his expert technical advice during this research and critical review of the manuscript.

NOMENCLATURE

A	Stratification parameter, $\left[\frac{MV_w^2}{2RT_0}\right]^{1/2}$
a	Outer rotor radius
$a_1, \ldots, a_6$	Integration constants
B	$ReS^{1/2}/4A^6$
DET	Determinant
$F(x, y)$	Source/sink in a simple cylinder
$F^*(x, y)$	Source/sink in an annulus
$\mathbf{f}^e$	Element load vector
$\mathbf{H}_3$	Cubic Hermite interpolating polynomial
$\mathbf{H}_5$	Quintic Hermite interpolating polynomial
$[\mathbf{K}^e]$	Element stiffness matrix
L	Rotor length
$L\chi$	$L_6\chi + B^2\chi_{yy}$
$L_6\chi$	$[e^x(e^x\chi_{xx})_{xx}]_{xx}$
$L_5\chi$	$[e^x(e^x\chi_{xx})_{xx}]_x$
$L_4\chi$	$[e^x(e^x\chi_{xx})_{xx}]$
$L_3\chi$	$(e^x\chi_{xx})_x$
l_x^e, l_y^e	Element width and height
M	Molecular weight
$\mathbf{N}^e$	Local element shape function
$\mathbf{N}^{eT}$	Transpose of local element shape function
Pr	Prandtl number
P	Perturbation pressure
R	Universal gas constant
Re	Wall Reynolds number
r	radial coordinate
r_i, r_o	inner (outer) radius
S	$1 + [(\gamma - 1)/2\gamma]PrA^2$
T_0	Reference temperature

u, v, w	Perturbation velocities
$\mathbf{u}^e$	Degrees of freedom
V_w	Wall speed
$\mathbf{w}^e$	Local element weight function
x	Scale heights variable
x_T	Gap width measured in scale heights
y	Dimensionless axial co-ordinate
β, β', β''	Slip coefficient
Γ	Computational domain
δ	Dimensionless gap width
$\partial\Gamma$	Closure
η	Dimensionless radius; element local axial co-ordinate
η_i	Dimensionless inner radius
θ	Temperature perturbation
ξ	Element local x-wise co-ordinate
ρ_0	Dimensionless zero order density, e^{-x}
$\sum_e$	Assembly algorithm
ϕ	$\theta - 2\omega$
χ	Master potential
Ω	Rotation rate
ω	Dimensionless angular velocity perturbation; global shape function
— (Overbar)	Boundary value

REFERENCES

1. H. Schlichting, *Boundary Layer Theory*, Sixth edn, McGraw-Hill Book Company, 1968.
2. H. P. Greenspan, *The Theory of Rotating Fluids*, Cambridge University Press, New York, 1968.
3. C. A. Jones, 'On flow between counter-rotating cylinders', *JFM*, **120,** 433–450 (1982).
4. T. Mullin, 'Mutations of steady cellular flows in the Taylor experiment', *JFM*, **121,** 207–218 (1982).
5. T. B. Benjamin and T. Mullin, 'Notes on the multiplicity of flows in the Taylor experiment', *JFM*, **121,** 219–230 (1982).
6. P. Bar-Yoseph, J. J. Blech, and A. Solan, 'Finite element solution of the Navier Stokes equations in rotating flow', *Int. j numer. methods eng.*, **17,** 1123–1146 (1981).
7. F. Bartels, 'Taylor vortices between two concentric rotating spheres', *JFM*, **119,** 1–26 (1982).
8. K. Nakabayshi, Y. Yamada and T. Kishimoto, 'Viscous frictional torque in the flow between two concentric rotating rough cylinders' *JFM*, **119,** 409–422 (1982).
9. L. Onsager, 'Approximate solutions of the linearized flow equations', unpublished manuscript (1965).
10. G. F. Carrier and S. Maslen, 'Flow phenomena in rapidly rotating systems', *USAEC Report TID-18065*, 1965.
11. A. T. Conlisk and J. D. A. Walker, 'Forced convection in a rapidly rotating annulus', *JFM*, **122,** 91–108 (1982).
12. A. T. Conlisk, M. R. Foster and J. D. A. Walker, 'Fluid dynamics and mass transfer in a gas centrifuge', *JFM*, **125,** 283–318 (1982).
13. A. T. Conlisk, M. R. Foster and J. D. A. Walker, 'Asymptotic theory of mass transfer in a gas centrifuge for small Ekman number', *Proceedings of Fifth Workshop on Gases in Strong Rotation*, 1983.
14. M. H. Berger, unpublished (1983).
15. E. Von Halle, 'The countercurrent gas centrifuge for the enrichment of U-235', Union Carbide Corporation Nuclear Division, Oak Ridge Gaseous Diffusion Plant, Oak Ridge, Tennessee, K/OA-4058, 1977.
16. H. G. Wood III and J. B. Morton, 'Onsager's pancake approximation for the fluid dynamics of a gas centrifuge', *JFM*, **101,** pt. 1, 1–31 (1980).
17. M. H. Berger, 'Analysis of gas flow in a centrifuge' *Ph.D. dissertation*, The University of Tennessee, Knoxville, 1982.
18. W. K. Sartory, Private communication, 1982.
19. F. Thomasset, *Implementation of Finite Element Methods for Navier–Stokes Equations*, Springer-Verlag, 1981.
20. G. N. Patterson, *Introduction to the Kinetic Theory of Gas Flows*, University of Toronto Press, 1971.
21. G. F. Malling, Private communication, 1982.
22. H. Lamb, *Hydrodynamics*, Sixth edn, Dover publications, 1945.
23. R. B. Bird, W. E. Stewart and E. N. Lightfoot, *Transport Phenomena*, Wiley, New York, 1960.

24. S. A. Schaaf and P. L. Chamber, *Flow of Rarefied Gases*, Princeton University Press, 1961.
25. W. G. May, 'Separation parameters of gas centrifuges', *AIChE Symposium Series*, **73**, (169), American Institute of Chemical Engineers, New York, 1977.
26. J. Durivault and P. Louvet, 'Etude theorique de l'ecoulement dans une centrifugeuse a contre courant thermique', *Rapport CEA-R-7414*, Centre D'Etudes Nucleaires de Saclay, 1976.